Adaptive Beamforming Applied to Medical Ultrasound Imaging

Johan-Fredrik Synnevåg, *Student Member, IEEE*, Andreas Austeng, *Member, IEEE*, and Sverre Holm, *Senior Member, IEEE*

***Abstract*—We have applied the minimum variance (MV) adaptive beamformer to medical ultrasound imaging and shown significant improvement in image quality compared to delay-and-sum (DAS). We demonstrate reduced mainlobe width and suppression of sidelobes on both simulated and experimental RF data of closely spaced wire targets, which gives potential contrast and resolution enhancement in medical images. The method is applied to experimental RF data from a heart phantom, in which we show increased resolution and improved definition of the ventricular walls.**

A potential weakness of adaptive beamformers is sensitivity to errors in the assumed wavefield parameters. We look at two ways to increase robustness of the proposed method; spatial smoothing and diagonal loading. We show that both are controlled by a single parameter that can move the performance from that of a MV beamformer to that of a DAS beamformer. We evaluate the sensitivity to velocity errors and show that reliable amplitude estimates are achieved while the mainlobe width and sidelobe levels are still significantly lower than for the conventional beamformer.

I. Introduction

Delay-and-sum (DAS) beamforming is the standard technique in medical ultrasound imaging. An image is formed by transmitting a narrow beam in a number of angles and dynamically delaying and summing the received signals from all channels. The sidelobe level of the DAS beamformer can be controlled using aperture shading, resulting in increased contrast at the expense of resolution. In contrast to the predetermined shading in DAS, adaptive beamformers use the recorded wavefield to compute the aperture weights. By suppressing interfering signals from off-axis directions and allowing large sidelobes in directions in which there is no received energy, the adaptive beamformers can increase resolution.

The minimum variance (MV) adaptive beamformer [1], [2] and subspace-based methods have mostly been studied in narrowband applications. Extensions to broadband imaging include preprocessing with focusing- and spatial-resampling filters, allowing narrowband methods to be used on broadband data [3], [4]. The MV beamformer has been applied to medical ultrasound imaging by several authors [5]–[9]. Mann and Walker [5] have used a constrained adaptive beamformer on experimental data of a single point-target and a cyst phantom demonstrating improved contrast and resolution. Sasso and Cohen-Bacrie [6] have applied a MV beamformer on a simulated dataset, showing improved contrast in the final image. Viola and Walker [9] have investigated use of several adaptive beamformers on simulated data and demonstrated improved resolution. Wang *et al.* [7] have applied a robust MV beamformer to medical ultrasound imaging using a synthetic aperture focusing approach. In their method, the spatial covariance matrix, which is required to find the optimal aperture shading, is calculated by averaging appropriately delayed data from each individual transmit element. Although this method allows dynamic focus on both transmission and reception, the loss in signal-to-noise ratio (SNR) caused by synthetic aperture focusing may be unacceptable in medical imaging applications. Also, data captured with different transmit elements may not be coherent due to target motion. In [8], we show preliminary results from the present method, in which full dynamic focus was applied through synthetic focus of individual transmitters. In this paper, we apply fixed focus on transmission. That allows us to evaluate the performance of the beamformer outside the transmit focal point, giving more realistic results for medical ultrasound imaging. We also consider ways of increasing the robustness of the MV beamformer, which ensures reliable amplitude estimates and at the same time improves performance.

In Section II, we present the method and show how robustness is achieved through either spatial smoothing or diagonal loading. In Section III we compare the MV beamformer to DAS on simulated and experimental RF data from closely spaced wire targets, and on experimental RF data of a heart phantom. We also evaluate the sensitivity of the method to errors in acoustic velocity and show that reliable amplitude estimates can be achieved by either of the robust methods. We discuss our findings in Section IV and draw conclusions in Section V.

II. Methods

A. Signal Model and Minimum Variance Beamformer

We assume an array of M elements, each recording a signal $x_m(t)$. We consider $P+1$ scatterers, each reflecting a signal, $s_p(t)$. We assume that $s_0(t)$ originates from the focal point of the receiver, and that the other reflectors are sources of interference. Under these assumptions, the mth time-delayed channel can be described as:

Manuscript received April 30, 2006; accepted October 18, 2006.

The authors are with the University of Oslo, Department of Informatics, Oslo, Norway (e-mail: johanfr@ifi.uio.no).

Digital Object Identifier 10.1109/TUFFC.2007.431

$$x_m(t) = \frac{1}{r_{m,0}} s_0(t) + \sum_{p=1}^{P} \frac{1}{r_{m,p}} s_p(t) * \delta(t - \tau_{m,p}) + n_m(t), \quad (1)$$

where $r_{m,p}$ is the distance from reflector p to sensor m, $\delta(t)$ is the Dirac delta-function, $\tau_{m,p}$ is the delay from reflector p to sensor m, $n_m(t)$ is noise on channel m, and $(*)$ is the convolution operator. The M observations are ordered in a vector:

$$\mathbf{X}(t) = \begin{bmatrix} x_0(t) \\ x_1(t) \\ \vdots \\ x_{M-1}(t) \end{bmatrix}, \quad (2)$$

which represents the observed wavefield. After delaying each channel to focus at a point in the image, the goal of the adaptive beamformer is to compute the optimal aperture shading before combining the channels. The output of the beamformer is a weighted sum of the spatial measurements:

$$z(t) = \sum_{m=0}^{M-1} w_m(t) x_m(t) = \mathbf{w}(t)^H \mathbf{X}(t), \quad (3)$$

where $w_m(t)$ is the aperture weight for sensor m, and $\mathbf{w}(t) = [w_0(t)\ w_1(t) \cdots w_{M-1}(t)]^H$. The minimum variance beamformer seeks to minimize the variance (power) of $z(t)$:

$$P(t) = E[|z(t)|^2], \quad (4)$$

while maintaining unit gain in the focal point. This optimization problem can be formulated as:

$$\begin{aligned} &\min_{\mathbf{w}(t)} \mathbf{w}(t)^H \mathbf{R}(t) \mathbf{w}(t), \\ &\text{subject to } \mathbf{w}(t)^H \mathbf{a} = 1, \end{aligned} \quad (5)$$

where:

$$\mathbf{R}(t) = E\left[\mathbf{X}(t)\mathbf{X}(t)^H\right], \quad (6)$$

is the spatial covariance matrix and $\mathbf{a}$ is the equivalent of the steering vector in narrowband applications. Because the data already have been delayed to focus at the point of interest, $\mathbf{a}$ is simply a vector of ones. The solution to (5) is:

$$\mathbf{w}(t) = \frac{\mathbf{R}(t)^{-1}\mathbf{a}}{\mathbf{a}^H \mathbf{R}(t)^{-1} \mathbf{a}}. \quad (7)$$

Applying these weights to (3) gives the MV amplitude estimate.

B. Estimation of the Spatial Covariance Matrix

In practice, the covariance matrix, $\mathbf{R}(t)$, in (7) is replaced by the sample covariance matrix, $\widehat{\mathbf{R}}(t)$. Because the transmitted pulses in medical ultrasound imaging are short and nonstationary, $\mathbf{R}(t)$ is rapidly changing with time. Hence, the estimate must be calculated from a single, or only a few, temporal samples. If synthetic aperture focusing (SAFT) is used as in [7], the estimate can be obtained by averaging the covariance matrices of appropriately delayed observations from each individual transmit element. Target motion and SNR requirements, however, may prohibit use of SAFT in practical medical ultrasound systems and require all elements to transmit simultaneously. To obtain a good estimate, we instead use spatial smoothing [10], in which the array is divided into overlapping subarrays, and the covariance matrices for all subarrays are averaged. This technique also is used to avoid signal cancellation in narrowband applications when sources are correlated or coherent. The estimated covariance matrix at time t then becomes:

$$\widehat{\mathbf{R}}(t) = \frac{1}{M - L + 1} \sum_{l=0}^{M-L} \overline{\mathbf{X}}_l(t) \overline{\mathbf{X}}_l^H(t), \quad (8)$$

where:

$$\overline{\mathbf{X}}_l(t) = \begin{bmatrix} x_l(t) \\ x_{l+1}(t) \\ \vdots \\ x_{l+L-1}(t) \end{bmatrix}, \quad (9)$$

and L is the subarray length. By using $\widehat{\mathbf{R}}(t)$ in (7) we see that the number of coefficients in $\mathbf{w}(t)$ is reduced, which limits the degrees of freedom to suppress interfering signals and noise. There is then a trade-off between accurate estimation of the covariance matrix and the length of the spatial filter. As we discuss in Section III, decreasing the subarray length leads to a more robust solution, but resolution is decreased.

After computation of the optimal aperture weights using the sample covariance matrix, we obtain the amplitude estimate as:

$$\hat{z}(t) = \frac{1}{M - L + 1} \sum_{l=0}^{M-L} \mathbf{w}(t)^H \overline{\mathbf{X}}_l(t). \quad (10)$$

The amplitude estimate can be viewed as a sum of $M - L + 1$ directive elements. Hence, the minimum variance solution approaches DAS as the subarray length is decreased. The overlapping subarrays give some more weight to the central elements, corresponding to a nonuniform shading.

C. Robust Minimum Variance Beamforming

Due to the high resolution of the MV beamformer at high SNR, a large number of scan lines may be required to avoid angular undersampling and to ensure robustness against errors in the wavefield parameters. We expect that such errors will affect the peaks in the amplitude estimates and lead to underestimation of the reflectivity of the targets. The constraint in (5) only assures that reflections originating from the focal point of the receiver are passed

with unit gain—others are suppressed. Wrong assumptions of acoustic velocity or phase aberrations will, for instance, lead to targets appearing slightly out of focus. The MV beamformer will try to minimize these reflections. By increasing robustness, we constrain the level of suppression outside the focal point, and allow reflections appearing slightly out of focus to pass through the beamformer.

We consider two ways to increase robustness of the proposed method in this paper; decreasing the subarray length when computing (8), and diagonal loading of the estimated covariance matrix. As discussed in Section II, the proposed method approaches the DAS beamformer as the subarray length, L, is decreased. In the extreme case where $L = 1$, (10) becomes the DAS solution with uniform aperture shading. Hence, by increasing the number of subarrays used to form the sample covariance matrix, we obtain an increasingly robust solution. However, increased robustness comes at the expense of resolution. The choice of subarray length should ensure that the covariance matrix estimate is invertible, which sets the upper limit on L to [11]:

$$L \leq M/2. \tag{11}$$

We show results for several values of L in Section III.

A second common way to increase robustness of the MV beamformer is to add a constant, ϵ, to the diagonal of the covariance matrix before evaluating (7). This means that $\widehat{\mathbf{R}}(t)$ is replaced by $\widehat{\mathbf{R}}(t) + \epsilon\mathbf{I}$. There exists several methods for calculating the value of ϵ based on the uncertainty in the model parameters [12]. We use a simple approach, in which the amount of diagonal loading is proportional to the power in the received signals [13]. We can view diagonal loading as adding spatially white noise to the recorded wavefield before computing the aperture weights. Increased noise level will constrain the sidelobe levels in directions in which there are no interfering signals, and thereby limit the level of suppression in directions in which interfering reflections appear. As white noise becomes dominant, the MV solution approaches the DAS beamformer with uniform shading. We can see this if we consider a wavefield of spatially white noise. The covariance matrix is then proportional to the identity matrix, $\mathbf{R}(t) = \sigma_n^2\mathbf{I}$, where σ_n^2 is the variance of the noise. From (7) we get:

$$\mathbf{w}(t) = \frac{(\sigma_n^2\mathbf{I})^{-1}\mathbf{a}}{\mathbf{a}^H(\sigma_n^2\mathbf{I})^{-1}\mathbf{a}} = \frac{\mathbf{a}}{\mathbf{a}^H\mathbf{a}} = \frac{1}{M}\mathbf{a}, \tag{12}$$

which is simply an unweighted sum of the elements. In the following results the amount of diagonal loading is found as:

$$\epsilon = \Delta \cdot \mathrm{tr}\{\widehat{\mathbf{R}}(t)\}, \tag{13}$$

where Δ is a constant and $\mathrm{tr}\{\cdot\}$ is the trace operator. The amount of diagonal loading then is given by the power in the received signals and the predetermined value Δ. Δ determines the relative weight given to the optimal solution in (7) and the DAS solution in (12). Setting $\Delta = 1/L$ corresponds to equal weighting of the two, in the sense that the traces of $\widehat{\mathbf{R}}(t)$ and $\epsilon\mathbf{I}$ are the same [13]. We also can interpret Δ as a parameter controlling the relative artificial noise level in the data. Setting $\Delta = 1/L$ corresponds to adding spatially white noise with the same average variance as the received signals. As we will see in Section III, we obtain a robust solution using $\Delta = 1/L$.

We now have two ways of increasing robustness of the proposed method, which both move the performance from that of a MV beamformer to that of an unweighted DAS beamformer.

III. Results

We have applied the MV beamformer to both simulated and experimental RF data and compared the results to the DAS beamformer. All transmitter and receiver combinations were simulated or recorded. The first processing steps were common to both beamformers: We synthesized fixed focus on transmission and dynamic focus on reception by delay and sum of the recorded data from each individual transmitter. Delays were implemented by upsampling the received signals and selecting the sample closest to the theoretically predicted delay. We then computed the discrete time analytic signal of each channel. This was done to avoid symmetric beampatterns in the MV solution, which could decrease resolution. The receiver channels then were summed for the DAS beamformer. For the MV beamformer, the optimal aperture weights were calculated and applied before summation. All MV beamformer results used subarray length $L \leq M/2$. Unless a diagonal loading parameter is given, we used $\Delta = 1/100L$ to ensure a well conditioned covariance matrix.

A. Simulated Data

We simulated an 18.5 mm, 96 element, 4 MHz transducer using Field II [14], imaging a number of pairwise reflectors located at depths 30–80 mm. The reflectors were separated by 2 mm. Transmit focus was 60 mm. We added white, Gaussian noise to each receiver channel before beamforming. SNR was approximately 40 dB per channel for the reflectors in focus.

Fig. 1(a) shows images obtained with the DAS and MV beamformers displayed over 55 dB dynamic range. Figs. 1(b)–(d) show the MV beamformer for different subarray lengths. We see that as L increases the reflectors are better resolved, whereas for smaller L the image is closer to DAS. Fig. 2 shows the steered responses at two different depths. Fig. 2(a) shows the reflectors at the focal point of the transducer and Fig. 2(b) shows the deepest reflectors. We see that there is a significant reduction in sidelobe level for the MV beamformer at both depths. Sidelobes rapidly decay toward the background noise level for all values of L, and they are between 15 and 20 dB lower than for DAS. We see that the mainlobe width decreases as subarrays

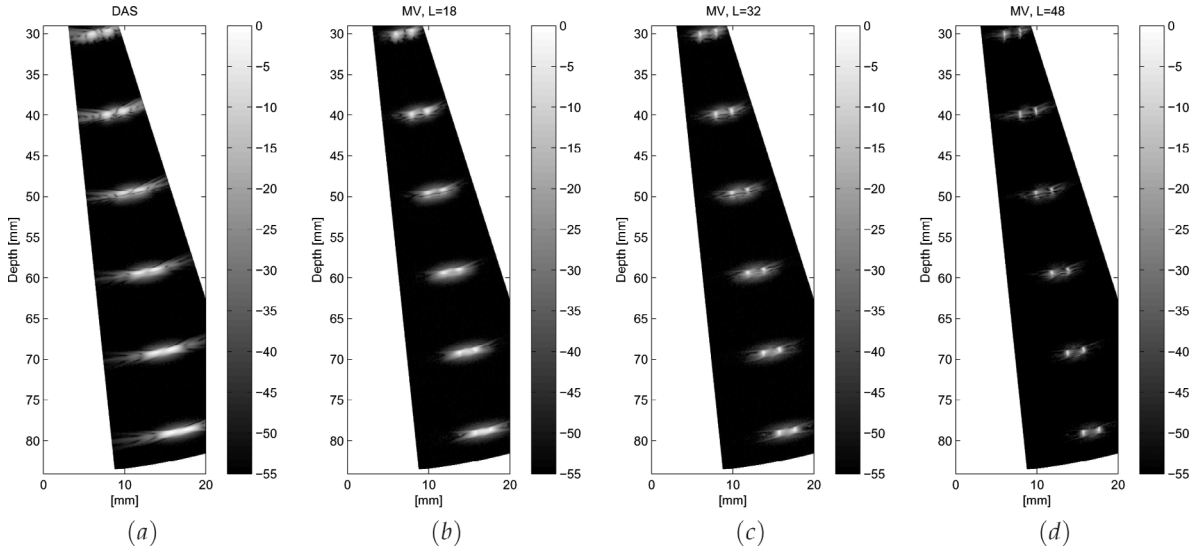

Fig. 1. Simulated wire targets using an 18.5 mm, 96 element, 4 MHz transducer. Transmit focus was 60 mm and dynamic receiver focus was applied. (a) DAS, (b) MV ($L = 18$), (c) MV ($L = 32$), and (d) MV ($L = 48$).

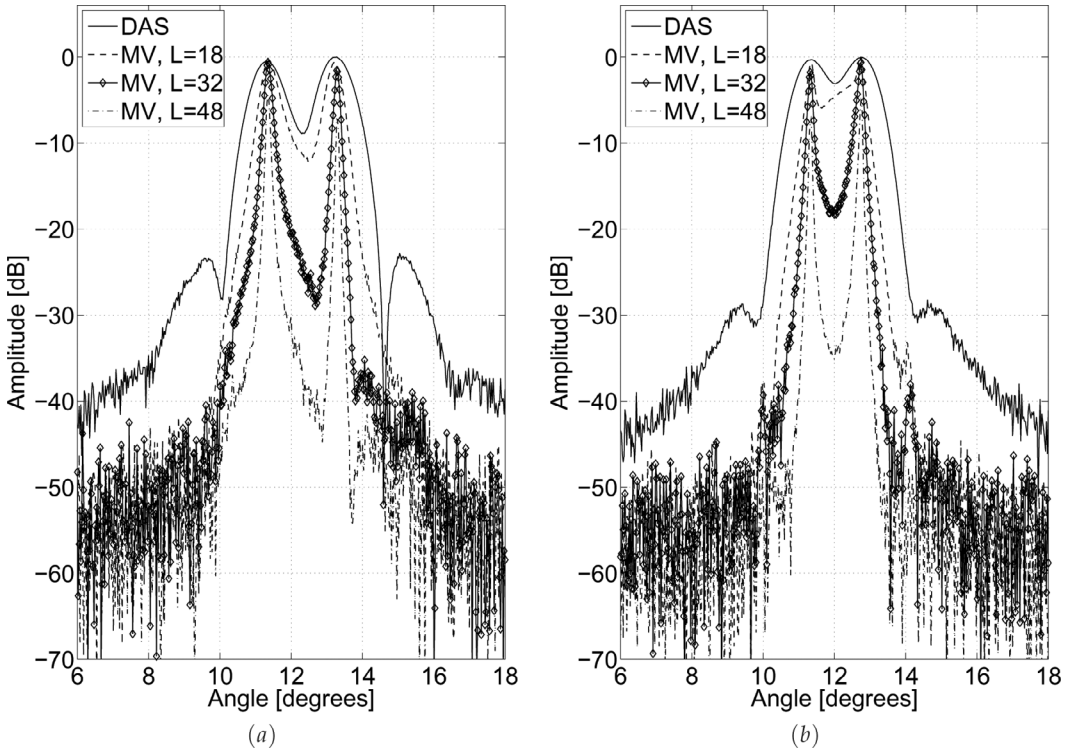

Fig. 2. Steered response of DAS and MV beamformers, using an 18.5 mm, 96 element, 4 MHz transducer, at depths (a) 60 mm and (b) 80 mm. Transmit focus was 60 mm and dynamic receiver focus was applied.

get longer. For the reflectors at the transmit focal point, the width is less than 1/4 of DAS for all examples. The wires are resolved by about 8 dB for DAS and up to 40 dB for MV. At 80 mm, which is away from the transmit focal point, DAS is unable to resolve the reflectors, and MV can resolve them by up to 30 dB. For $L = 18$, the MV beamformer is unable to separate the reflections, but the sidelobes are still about 20 dB lower, giving better definition of edges.

B. Sensitivity to Velocity Errors

As mentioned, a potential weakness of adaptive beamformers is lack of robustness against errors in the assumed wavefield parameters. The following results show the MV beamformers' sensitivity to errors in acoustic velocity for the different robust methods. We used the same simulated data as in Section II, and beamformed the data with overestimation of the acoustic velocity by 5%. An error of this

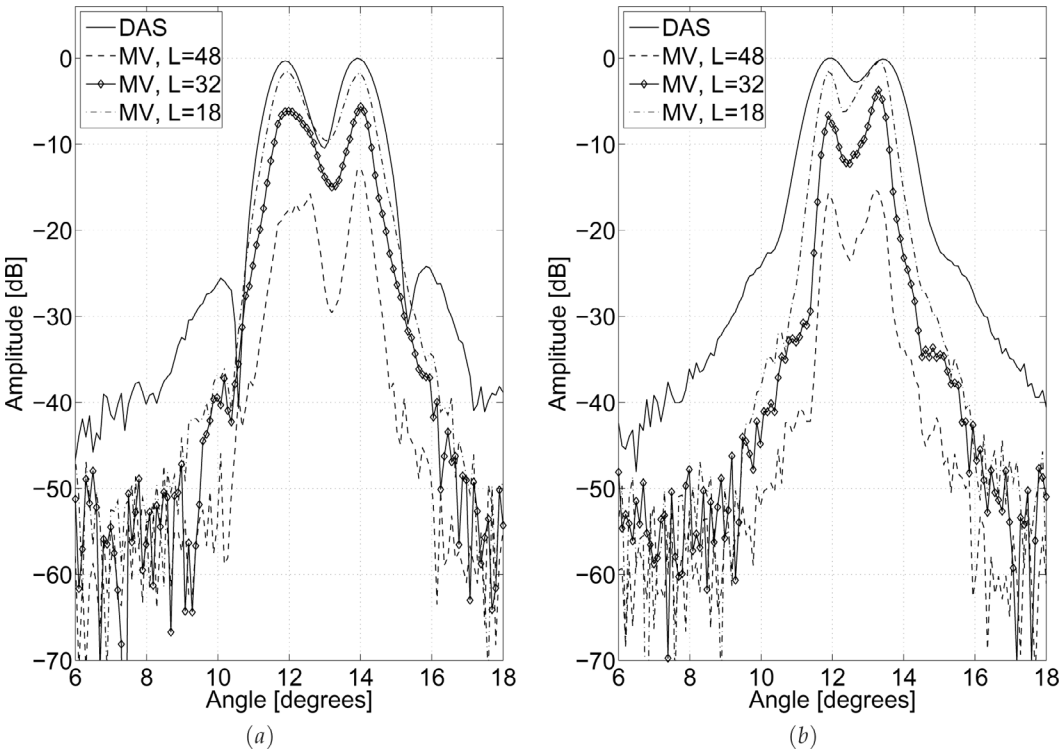

Fig. 3. Steered response of DAS and MV beamformers, using an 18.5 mm, 96 element, 4 MHz transducer in which images were formed with 5% error in acoustic velocity: (a) 60 mm and (b) 80 mm depth. Transmit focus was 60 mm and dynamic receiver focus was applied.

size covers the uncertainty in medical ultrasound imaging, in which the acoustic velocities range from about 1440 m/s in fat to about 1570 m/s in blood [15]. Fig. 3 shows the steered response at depths 60 and 80 mm for DAS and MV for different subarray lengths. For $L = 48$, we see that the peak amplitudes are grossly underestimated at both depths, due to the high level of suppression of reflections appearing out of focus. We also see that, as the subarray length is decreased, the MV amplitude estimates approach those of DAS. For $L = 18$ at 60 mm, the mainlobe width is approximately the same as DAS, but the sidelobes are about 12 dB lower. At 80 mm, the mainlobe width is narrower as well, and the amplitude estimates are approximately the same.

Fig. 4 shows corresponding results for different amounts of diagonal loading. We see that, as the regularization parameter, Δ, increases, the MV amplitude estimates approach those of DAS. As for spatial smoothing, diagonal loading trades off mainlobe width for robustness in the amplitude estimates. Again, the sidelobe level for all examples of Δ is significantly lower than for DAS.

C. Experimental Data: Wire Targets

We recorded experimental RF data with a specially programmed System FiVe scanner (GE Vingmed Ultrasound, Horten, Norway) using an 18.5 mm, 96 element, 3.5 MHz transducer driven at 4 MHz. The data were sampled at 20 MHz and upsampled by a factor 8 before delays were applied. The wires were separated by 2 mm. We used subarray length, $L = 48$ and $\Delta = 1/L$ for the MV beamformer. Fig. 5 shows the steered responses of the DAS and MV beamformers at two different depths, for which the latter is at the transmit focal point. We see that the sidelobes are significantly lower for the MV beamformer. In Fig. 5(a), which is away from the focal point, the mainlobe width is only slightly narrower due to the high amount of diagonal loading. At the focal point in Fig. 5(b), the mainlobe width also is reduced, demonstrating improved performance on experimental data.

D. Experimental Data: Heart Phantom

The demonstrated properties of the MV beamformer on wire targets should lead to improved contrast and resolution in medical ultrasound images. We applied the method to experimental RF data from a heart phantom. The data-set was obtained from the Biomedical Ultrasound Laboratory, University of Michigan[1]. Data were recorded with a 64 element, 3.33 MHz transducer, and sampled at 17.76 MHz. Data were upsampled by a factor 8 before delays were applied. We used subarray length $L = 32$, and diagonal loading with $\Delta = 1/10L$ for the MV beamformer. Transmit focus was 60 mm. Fig. 6 shows the images obtained with the DAS and MV beamformers displayed over 55 dB dynamic range. We see that the resolution in general is much better in the MV image. We also see that the

[1]Ultrasound RF data-set heart from the Biomedical Ultrasonic Laboratory, University of Michigan, Apr. 2006. Available at http://bul.eecs.umich.edu/, April 2006.

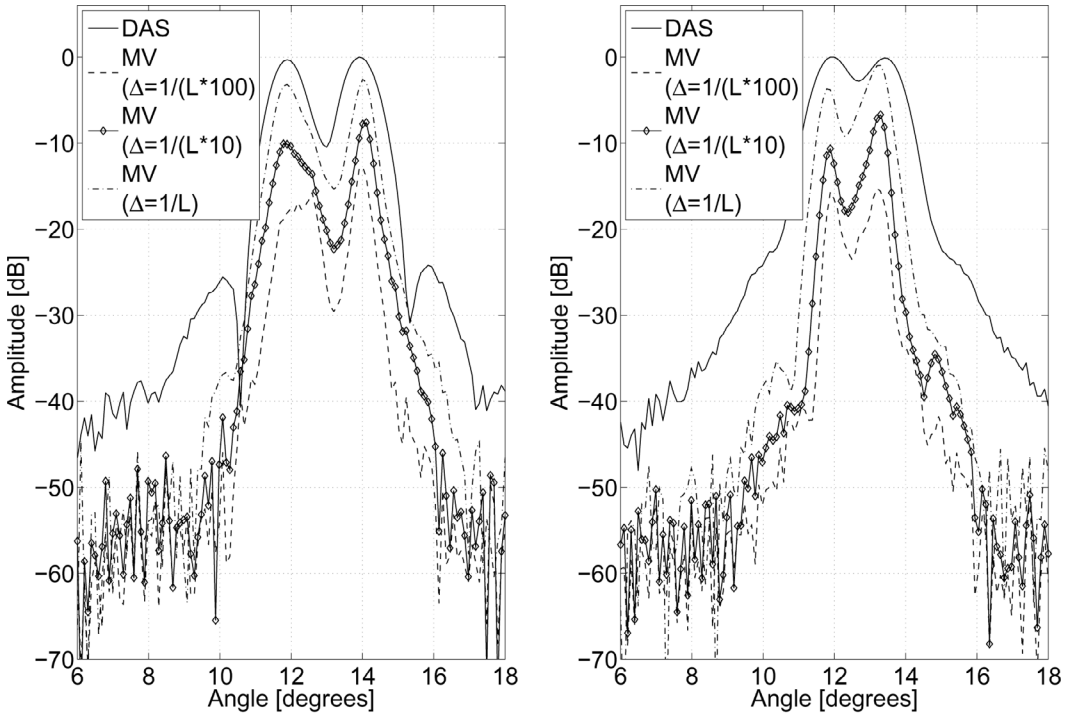

Fig. 4. Steered response of DAS and MV beamformers with different amount of diagonal loading, using an 18.5 mm, 96 element, 4 MHz transducer: (a) 60 mm and (b) 80 mm depth. Images were formed with 5% error in acoustic velocity. Transmit focus was 60 mm and dynamic receiver focus was applied.

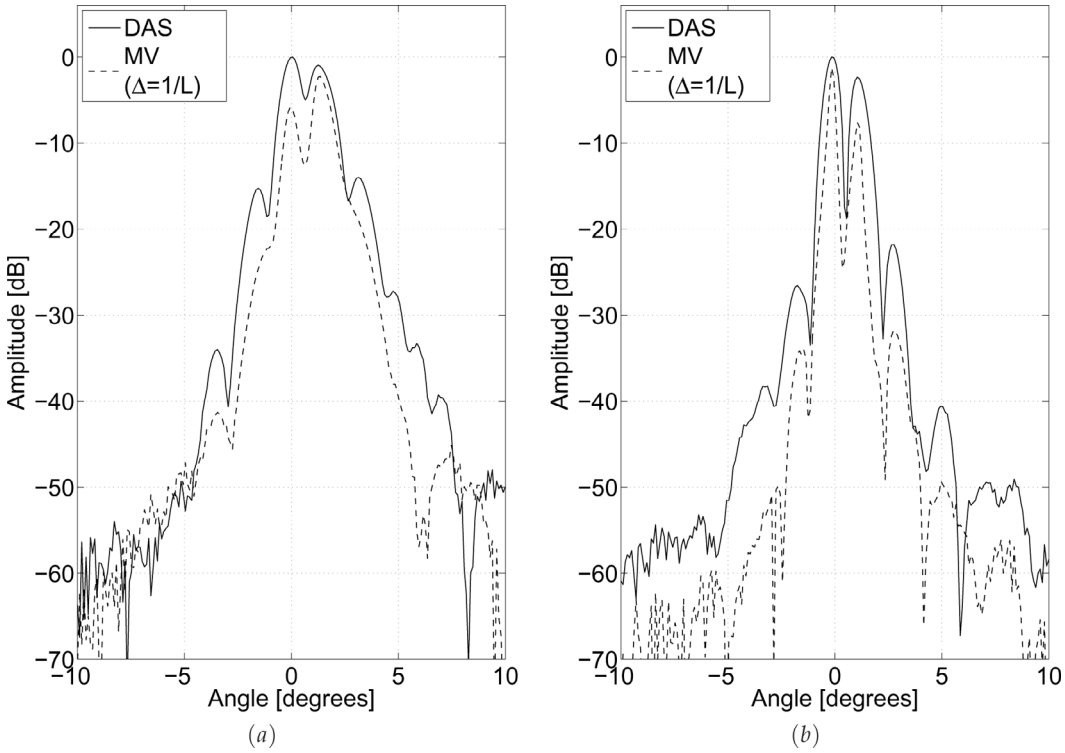

Fig. 5. Steered response of DAS and MV beamformers applied to experimental RF data, using an 18.5 mm, 96 element, 3.5 MHz transducer driven at 4 MHz: (a) 46 mm and (b) 56 mm depth. Transmit focus was 56 mm and dynamic receiver focus was applied.

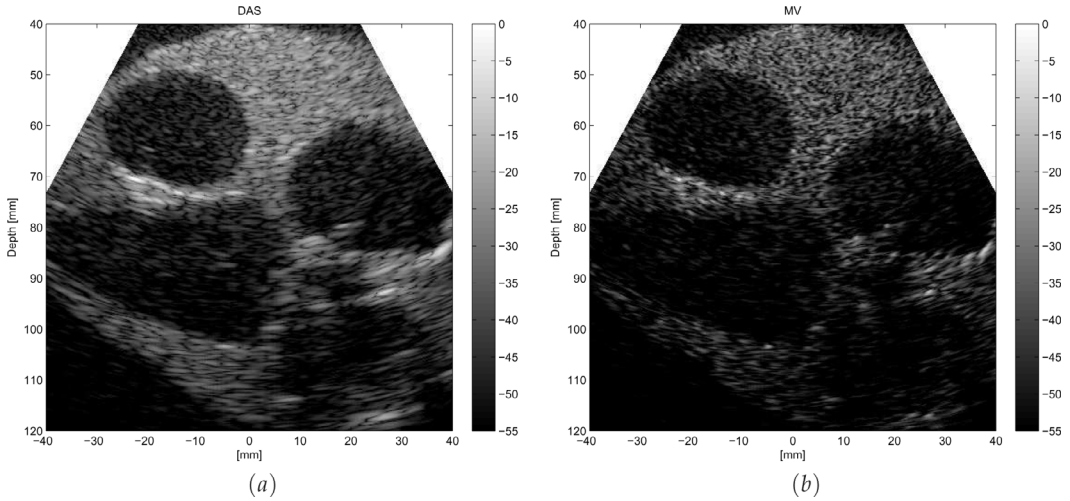

Fig. 6. Images obtained from experimental RF data from a heart-phantom using a 15.4 mm, 64 element, 3.33 MHz transducer: (a) DAS and (b) MV with $L = 32$ and $\Delta = 1/10L$. Transmit focus was 60 mm and dynamic receiver focus was applied.

definition of the ventricular walls is improved, owing to the narrow beam and low sidelobe level.

IV. Discussion

The performance of the MV beamformer is dependent on the SNR. As SNR decreases, resolution will decrease in a manner similar to increasing the amount of diagonal loading. However, from (12) we see that in the absence of model-errors, the MV beamformer will perform equal to or better than the unshaded DAS, provided that images are formed with sufficient angular sampling. Figs. 1 and 2 show that the MV beamformer achieved much higher resolution and lower sidelobes than DAS for $L = M/2$. Also, as subarray length was decreased, the resolution approached that of DAS. Still, the sidelobes were significantly lower than for DAS for all examples of L.

The results in Figs. 3 and 4 confirms that the MV beamformer underestimates the amplitudes of the reflected signals in the presence of wavefield perturbations. By decreasing the subarray length or applying diagonal loading, reliable amplitude estimates were achieved; but the ability to resolve the targets was affected. We see from the figures that the main trade-off when choosing values for L and Δ is between mainlobe width and robustness. Sidelobes were significantly lower than DAS for all examples of these parameters.

Setting $L = 18$ for the 96 element transducer in Fig. 3 gave amplitudes close to DAS, but resolution was only slightly improved. Using $L = M/2$ and $\Delta = 1/L$ in Fig. 4 gave similar results. A velocity shift of 5%, however, may be more than the typical estimation error. Beamforming the experimental heart-phantom data in Fig. 6 gave good results using $L = M/2$ and $\Delta = 1/10L$, in the sense that resolution was improved and the peak amplitudes in the images for DAS and MV were approximately the same.

The improved performance of the MV beamformer comes at a computational cost. As the delay-step is common to both beamformers, the computational overhead comes from calculation and application of the aperture weights. The computational complexity of direct computation of (7) is approximately $O(L^3)$. Increasing robustness using shorter subarrays, therefore, has a computational advantage over diagonal loading.

V. Conclusions

We have successfully applied the minimum variance beamformer to medical ultrasound imaging and shown significant performance improvement compared to DAS. Results have been demonstrated on both simulated and experimental RF data. We have demonstrated two ways of increasing robustness of the method, which can give reliable amplitude estimates while still improving resolution and contrast. The method was applied to RF data from a realistic image, and showed significant improvement in image quality.

References

[1] F. Bryn, "Optimum signal processing of three-dimensional arrays operating on Gaussian signals and noise," *J. Acoust. Soc. Amer.*, vol. 34, no. 3, pp. 289–297, Mar. 1962.

[2] J. Capon, "High-resolution frequency-wavenumber spectrum analysis," *Proc. IEEE*, vol. 57, pp. 1408–1418, Aug. 1969.

[3] J. Krolik and D. Swingler, "The performance of minimax spatial resampling filters for focusing wide-band arrays," *IEEE Trans. Signal Processing*, vol. 39, no. 8, pp. 1899–1903, Aug. 1991.

[4] S. Sivanand, J.-F. Yang, and M. Kaveh, "Focusing filters for wide-band direction finding," *IEEE Trans. Signal Processing*, vol. 39, no. 2, pp. 437–445, Feb. 1991.

[5] J. A. Mann and W. F. Walker, "A constrained adaptive beamformer for medical ultrasound: Initial results," in *Proc. IEEE Ultrason. Symp.*, 2002, pp. 1807–1810.

[6] M. Sasso and C. Cohen-Bacrie, "Medical ultrasound imaging using the fully adaptive beamformer," in *Proc. IEEE Int. Conf. Acoust. Speech Signal Processing*, Mar. 2005, pp. 489–492.

[7] Z. Wang, J. Li, and R. Wu, "Time-delay- and time-reversal-based robust Capon beamformers for ultrasound imaging," *IEEE Trans. Med. Imag.*, vol. 24, pp. 1308–1322, Oct. 2005.

[8] J.-F. Synnevåg, A. Austeng, and S. Holm, "Minimum variance adaptive beamforming applied to medical ultrasound imaging," in *Proc. IEEE Ultrason. Symp.*, 2005, pp. 1199–1202.
[9] F. Viola and W. F. Walker, "Adaptive signal processing in medical ultrasound beamforming," in *Proc. IEEE Ultrason. Symp.*, 2005, pp. 1980–1983.
[10] T.-J. Shan, M. Wax, and T. Kailath, "On spatial smoothing for direction-of-arrival estimation of coherent signals," *IEEE Trans. Acoust. Speech Signal Processing*, vol. 33, no. 4, pp. 806–811, Aug. 1985.
[11] P. Stoica and R. Moses, *Introduction to Spectral Analysis*. Englewood Cliffs, NJ: Prentice-Hall, 1997.
[12] J. Li, P. Stoica, and Z. Wang, "On robust Capon beamforming and diagonal loading," *IEEE Trans. Signal Processing*, vol. 51, no. 7, pp. 1702–1715, July 2003.
[13] A. Ozbek, "Adaptive seismic noise and interference attenuation method," U.S. Patent No.: US 6,446,008 B1, Sep. 2002.
[14] J. A. Jensen, "Field: A program for simulating ultrasound systems," *Med. Biol. Eng. Comput.*, vol. 34, pp. 351–353, 1996.
[15] B. A. J. Angelsen, *Ultrasound Imaging. Waves, Signals and Signal Processing*. Trondheim, Norway: Emantec, 2000.

Johan-Fredrik Synnevåg (S'06) was born in Bergen, Norway, in 1974. He received the M.S. degree in computer science from the University of Oslo, Oslo, Norway, in 1998. From 1999 to 2004 he worked as a project engineer in Schlumberger (now WesternGeco), Asker, Norway. He is currently pursuing a Ph.D. degree in signal processing at the University of Oslo.

His research interests include array signal processing.

Andreas Austeng (S'97–M'02) was born in Oslo, Norway, in 1970. He received the M.S. degree in physics in 1996 and the Ph.D. degree in computer science in 2001, both from the University of Oslo, Oslo, Norway. Since 2001 he has been working at the Department on Informatics, University of Oslo, first as a postdoctoral research fellow, and currently as an associate professor.

His research interests include signal processing for acoustical imaging.

Sverre Holm (M'82–SM'02) was born in Oslo, Norway, in 1954. He received the M.S. and Ph.D. degrees in electrical engineering from the Norwegian Institute of Technology, Trondheim, in 1978 and 1982.

He has done research and development in speech coding and frequency estimation at SINTEF, Trondheim, Norway, and worked with synthetic aperture radar processing and spectral estimation at Informasjonskontroll AS, Asker, Norway. From 1990 to 1994 he was at GE Vingmed Ultrasound, Horten, Norway, doing research and development work in digital beamforming, ultrasound probes, and ultrasound contrast agents. He spent the fall of 1998 on a sabbatical at GE Global Research, Schenectady, NY.

He has been an assistant professor in the Electrical Engineering Department of Yarmouk University in Jordan (1984–1986) and from 1989 he was an adjunct professor, until 1992 at the Norwegian Institute of Technology, then at the University of Oslo, Oslo, Norway. Since 1995 he has been a full professor of signal processing at the University of Oslo working in ultrasound and sonar imaging, acoustic field simulation, and indoor positioning systems.

Dr. Holm was an associate editor of the *IEEE Transactions on Ultrasonics, Ferroelectrics, and Frequency Control* from 1997–2002. He was elected as a member of the Norwegian Academy of Technological Sciences in 2002.